Published in final edited form as:
Eur J Neurosci. 2009 October ; 30(7): 1239–1250. doi:10.1111/j.1460-9568.2009.06924.x.

Lateral Habenula Projections to the Rat Ventral Tegmental Area: Sparse Synapses Observed Onto Dopamine and GABA Neurons

Natalia Omelchenko[1], **Roland Bell**[1], and **Susan R. Sesack**[1,2,*]

[1] Department of Neuroscience, University of Pittsburgh, Pittsburgh, PA 15260

[2] Department of Psychiatry, University of Pittsburgh, Pittsburgh, PA 15260

Abstract

Ventral tegmental area (VTA) dopamine (DA) neurons and their forebrain projections are critically involved in reward processing and cognitive functions. Descending projections from the lateral habenula (LHb) play a central role in inhibiting DA cell activity in response to the absence of expected rewards. As LHb efferents are reportedly glutamatergic, their ability to inhibit DA cells would theoretically require a disynaptic connection involving VTA GABA neurons and their local collateral inputs to DA cells. To test this hypothesis, anterograde tract-tracing from the LHb was used to investigate the relative selectivity of LHb synapses onto GABA versus DA VTA neurons. LHb axons were visualized using immunoperoxidase, and DA and GABA cells were marked by immunogold-silver labeling for tyrosine hydroxylase (TH) or GABA, respectively. By ultrastructural analysis, 16% of LHb axons were observed to form synaptic contacts in the VTA, and most of these were of an intermediate morphological type that did not exhibit definitive asymmetric or symmetric character. LHb axons targeted TH- and GABA-labeled dendrites to a comparable extent (45% and 52% observed incidence, respectively). Preembedding immunogold labeling for the vesicular glutamate transporter type 2 and postembedding immunogold staining for GABA confirmed that approximately 85% of LHb terminals were glutamatergic and not GABAergic. These results suggest that the robust inhibition of DA cells evoked by the LHb is unlikely to arise from a selective innervation of VTA GABA neurons. Moreover, the LHb may mediate a direct excitation of DA cells that is over-ridden by indirect inhibition originating from an extrinsic source.

Keywords

glutamate; ultrastructure

Dopamine (DA) neurons in the ventral tegmental area (VTA) project to a number of forebrain targets and critically modulate motivated behaviors and cognitive functions (Koob, 1996; Overton & Clark, 1997; Schultz, 1998; Redgrave *et al.*, 1999). Performance of these functions is associated with changes in DA cell activity and DA efflux in target areas (Brozoski *et al.*, 1979; Watanabe *et al.*, 1997; Schultz, 1998; Redgrave *et al.*, 1999; Stefani & Moghaddam, 2006). The firing patterns exhibited by DA cells include tonic pacemaker-like activity superimposed by bursts and pauses that reflect excitatory and inhibitory afferents, respectively (White, 1996; Overton & Clark, 1997; Kitai *et al.*, 1999; Grace *et al.*, 2007; Tepper & Lee, 2007). DA cells fire short bursts in response to unpredicted rewards and novel stimuli, whereas inhibitory pauses are evoked by the absence of expected rewards and by aversive events (Horvitz *et al.*, 1997; Schultz, 1998; Ungless *et al.*, 2004). This activity pattern is consistent

*Correspondence to: Susan R. Sesack, PhD, Department of Neuroscience, Langley Hall, Room 210, University of Pittsburgh, Pittsburgh, PA 15260, Voice: (412) 624-5158, Fax: (412) 624-9198, sesack@pitt.edu.

with DA's role in promoting behaviors that are reinforced and attenuating behaviors with negative consequences. Understanding the morphological bases of behavioral control requires characterizing the afferents that regulate firing patterns in midbrain DA neurons, including those that depress activity when rewards are worse than predicted.

A potentially important afferent to the VTA arises from the lateral habenula (LHb), an epithalamic region that directs information from limbic and basal ganglia structures toward brainstem monoamine centers and that reportedly contributes to reproductive, maternal and stress behaviors (Klemm, 2004; Hikosaka, 2007; Geisler & Trimble, 2008; Hikosaka *et al.*, 2008). A crucial role for the LHb in reinforcement learning was recently shown in behaving primates in which LHb cells were inhibited by stimuli predicting reward and excited by stimuli predicting no reward (Matsumoto & Hikosaka, 2007). The pattern of LHb cell activity is the inverse of DA neuron firing under the same conditions, and the activation of the LHb to no reward precedes DA cell inhibition (Matsumoto & Hikosaka, 2007). This temporal correlation of LHb firing with inverted responses in midbrain DA cells suggests that the LHb is at least partly responsible for inducing pauses in DA cell activity patterns. This supposition is supported by electrophysiological studies reporting consistent, short-latency inhibitory responses in DA neurons following electrical stimulation of the LHb (Christoph *et al.*, 1986; Ji & Shepard, 2007; Matsumoto & Hikosaka, 2007). LHb activation also reduces extracellular DA levels in the forebrain, whereas reduced habenular outflow increases DA levels (Lisoprawski *et al.*, 1980; Lecourtier *et al.*, 2008).

A projection from the LHb to the VTA has been shown by numerous tract-tracing studies (Herkenham & Nauta, 1979; Araki *et al.*, 1988; Geisler & Zahm, 2005; Geisler *et al.*, 2007; Kim, 2009). Nevertheless, the synaptic organization of this pathway remains to be established. Phenotypic data indicates that the majority of LHb neurons (including cells that innervate the VTA) are glutamatergic and therefore excitatory (Kalen *et al.*, 1985; Matsuda & Fujimura, 1992; Fremeau *et al.*, 2001; Herzog *et al.*, 2004; Geisler *et al.*, 2007; Aizawa *et al.*, 2008). Hence, the dominant and consistent inhibitory influence of the LHb on DA cell activity indicates that these effects are almost certainly polysynaptic. These observations give rise to a relatively simple circuit hypothesis, namely that LHb cells form selective excitatory synapses onto VTA GABA neurons and these in turn inhibit DA cells through local collaterals (Phillipson, 1979; Johnson & North, 1992; Nugent & Kauer, 2008; Omelchenko & Sesack, 2009). Such disynaptic connections have been invoked previously to explain paradoxical excitatory or inhibitory responses of midbrain DA cells to activation of inhibitory or excitatory afferents, respectively (Grace & Bunney, 1985; Smith & Grace, 1992; Tong *et al.*, 1996; White, 1996; Tepper & Lee, 2007).

We sought to address this hypothesis in rats by combining tract-tracing from the LHb with immunocytochemistry for markers of DA and GABA neurons. Examination of the tissue by electron microscopy was used to identify the synaptic contacts and phenotypes of LHb axons. Some of the preliminary data were presented in an abstract (Bell *et al.*, 2007) and a symposium related mini-review (Hikosaka *et al.*, 2008).

Materials and Methods

Subjects and surgeries

All procedures involving animals were conducted in accordance with the NIH Guide for the Care and Use of Laboratory Animals and were approved by the Institutional Animal Care and Use Committee at the University of Pittsburgh. Thirteen adult male Sprague-Dawley rats (Hilltop Lab Animals, Scottdale, PA, 260–400g) were anesthetized with a mixture of drugs (34 mg/kg ketamine, 1 mg/kg acetopromazine, and 7 mg/kg xylazine) injected i.m. Rats were placed in a stereotaxic apparatus, and the anterograde tracer *Phaseolus vulgaris* leucoagglutinin

(PHAL; Vector Laboratories, Burlingame, CA) was injected into the LHb in one hemisphere (one animal in the study received bilateral injections). PHAL was injected iontophoretically as a 2.5% solution in 10 mM sodium phosphate buffer by passing anodal current (+5 μA pulsed 10 seconds on/off) for 20 minutes through glass micropipettes with 10–20 μm tip diameters. Injections were made at the following coordinates: 3.2 mm posterior to bregma, 1 mm lateral to midline, and 5.0–5.1 mm ventral to the skull surface.

Following a survival period that ranged from 4–30 days, rats were anesthetized with an i.p. injection of pentobarbital at a dose of 60 mg/kg followed by supplemental injections as needed. Rats also received a zinc chelator to prevent false silver enhancement of endogenous zinc (Veznedaroglu & Milner, 1992). For this purpose, animals received i.p. injections of 1g/kg diethyldithiocarbamic acid (Sigma, St. Louis, MO) 15 minutes before they were sacrificed.

In 7 animals, intracardial perfusions were initiated with heparin saline (Elkins-Sinn, Cherry Hill, NJ; 1,000 U/ml), followed by 50 ml of 3.75% acrolein plus 2% paraformaldehyde in 0.1M phosphate buffer, pH 7.4 (PB), and then followed by 250–500 ml of 2% paraformaldehyde. The remaining 6 animals were sacrificed by perfusion with heparin saline, followed by 2% paraformaldehyde and 1% glutaraldehyde in PB. The brain tissue from these animals was used for postembedding immunolabeling for GABA. In all cases, the extracted brains were post-fixed in 2% paraformaldehyde for 0.5 to 1 hour before being switched to 0.1M PB. Brains were blocked into thick sections containing all of the VTA and LHb, and then sectioned further at 50 μm on a Vibratome. Free-floating sections were collected in PB, and then exposed to 1% sodium borohydride in PB for 30 minutes so as to reduce cross-linking of antigens and enhance antibody labeling.

Preembedding immunocytochemistry

In order to characterize the projection targets of LHb terminals in the VTA, immunoperoxidase labeling for PHAL was developed in combination with preembedding immunogold-silver labeling for tyrosine hydroxylase (TH) in DA neurons or for GABA. The neurotransmitter phenotype of PHAL-containing terminals was identified by preembedding immunogold-silver labeling for PHAL in combination with either preembedding immunoperoxidase labeling for the vesicular glutamate transporter type 2 (VGlut2) (Bellocchio *et al.*, 1998; Fremeau *et al.*, 2001) or postembedding immunogold staining for GABA (see below). As expected for a subcortical structure, VGlut2 is the dominant vesicular glutamate transporter expressed in the LHb (Herzog *et al.*, 2004; Geisler *et al.*, 2007)

All of these antibodies have been used extensively in our prior studies (Carr & Sesack, 2000; Omelchenko & Sesack, 2005; 2007; Omelchenko & Sesack, 2009). The mouse monoclonal TH antibody (Chemicon #MAB318, Temecula, CA) was raised against an N-terminal protein from the TH molecule purified from PC12 cells and has been shown by Western blot analysis to label a single band of 59–61 kDA and to specifically recognize TH and not other monoamine synthetic enzymes (Wolf & Kapatos, 1989). The mouse monoclonal GABA antibody (Sigma #A-0310) was developed against GABA conjugated to bovine serum albumin (BSA). This antibody has been shown by the manufacturer to bind to GABA and not several closely related amino acids. Moreover, this antibody consistently labels axon terminals forming symmetric and rarely asymmetric synapses (Carr & Sesack, 2000; Omelchenko & Sesack, 2005; 2007; Omelchenko & Sesack, 2009). We have also demonstrated that the monoclonal anti-GABA antibody labels axon terminals in the VTA that display additional postembedding immunoreactivity for GABA detected by a different antibody (Omelchenko & Sesack, 2009). Specificity of the guinea pig polyclonal antibody against VGlut2 (Chemicon, #23041014) was demonstrated by the manufacturer using Western blot analysis on rat brain lysate. Further evidence for specificity has been shown by preadsorption controls in astrocytic preparations, which were also used to demonstrate that the VGlut2 antibody does not cross react with VGlut3

(Montana *et al*., 2004). For the rabbit antibody against PHAL (Vector, Burlingame, CA), specificity is demonstrated by the absence of immunoreactivity from brain regions that do not receive projections from the LHb where this tracer was injected.

Sections were rinsed several times in 0.1M Tris-buffered saline, pH 7.6 (TBS) and then processed separately for light and electron microscopic analysis. Sections for electron microscopy were placed for 30 minutes in a blocking solution comprised of 1% bovine serum albumin and 3% normal donkey serum in 0.1 M TBS containing 0.04% Triton X-100 (Sigma). Light microscopic sections were exposed to the same blocking solution containing 0.2% Triton X-100. Sections were singly-labeled for PHAL or dually-labeled for PHAL in combination with TH, GABA or VGlut2 using an overnight incubation in the blocking solution that contained rabbit anti-PHAL (1:1,000) with or without mouse anti-TH (1:5,000), mouse anti-GABA (1:1,000), or guinea pig anti-VGlut2 (1:16,000) antibodies.

For immunoperoxidase labeling, sections were rinsed and placed in the same blocking solution containing biotinylated goat anti-rabbit IgG (1:400; Vector Labs) for 30 minutes. Sections were then rinsed in TBS and placed in a 1:100 dilution of avidin-biotin peroxidase complex (Vectastain Elite kit; Vector Labs) for 30 minutes. A 3.5 minute incubation in TBS containing 0.02% diaminobenzidine (Sigma) and 0.003% hydrogen peroxide was used to visualize the peroxidase-labeled antibodies. Sections were then rinsed multiple times in TBS to stop the reaction.

Sections were prepared for immunogold-silver labeling for PHAL, TH or GABA with a 30 minute incubation in a washing buffer (0.8% bovine serum albumin, 0.1% fish gelatin, and 3% normal donkey serum in 10 mM phosphate buffered saline, pH 7.4; PBS). The tissue was placed overnight in a 1:50 mixture of 1 nm gold-conjugated goat anti-mouse or goat anti-rabbit IgG (Electron Microscopy Sciences, Hatfield, PA) in the same blocking solution. Sections were then rinsed multiple times first in this blocking solution and then in PBS. Post-fixation in 2% glutaraldehyde in PBS was then performed followed by subsequent rinses in PBS and then a 0.2 M sodium citrate buffer, pH 7.4. Gold particles conjugated to the secondary antibodies were then enlarged with a 4–6 minute incubation step in a silver-enhancement solution (GE Healthcare Life Sciences).

Tissue preparation for light and electron microscopy

Sections prepared for analysis by light microscopy as described above were mounted onto glass slides and then dehydrated through an ethanol gradient, followed by xylene. Slides were then coverslipped using a DPX mounting-medium. An Olympus BX51 microscope and Orca Hamamatsu digital camera were used to capture photomicrographs of brain sections. Adobe Photoshop (SanJose, CA) was then used to adjust captured images to maintain consistency in contrast and exposure between images. A one hour incubation in 2% osmium tetroxide in PB was used to render membranes electron-dense. Graded alcohol solutions followed by propylene oxide were used to dehydrate these sections, which were then flat-embedded in epoxy resin (EM bed 812; Electron Microscopy Sciences) between sheets of commercial polymer film.

A Leica Ultracut was used to collect ultrathin sections from the anterior to middle VTA (−4.8 to −5.8 posterior to bregma). Between 2 and 7 serial ultrathin sections were collected onto copper or nickel mesh grids and then counterstained with uranyl acetate and lead citrate. All sections prepared in this way were examined on a FEI Morgagni transmission electron microscope (Hillsboro, Oregon) and captured with an XR-60 digital microscope from Advanced Microscopy Techniques (Danvers, MA). Adobe Photoshop was again used to adjust contrast and exposure.

Postembedding immunocytochemistry

Although the preembedding method works well for labeling GABA in dendrites (Van Bockstaele & Pickel, 1995), postembedding provides the most sensitive means for detecting GABA in axons (Smith *et al.*, 1996; Bokor *et al.*, 2005; Omelchenko & Sesack, 2009). In the present study, postembedding labeling was performed utilizing a procedure modified from Smith and colleagues (Shink & Smith, 1995; Smith *et al.*, 1996) and recently described in detail by our laboratory (Omelchenko & Sesack, 2009). This method was applied to tissue sets where PHAL was detected by single-label preembedding immunogold that was silver-enhanced to create particles substantially larger than those associated with postembedding gold labeling for GABA. The specificity of the rabbit anti-GABA antibody (Sigma, A-2052) used for postembedding was demonstrated in dot blot assay by the manufacturer and has also shown excellent specificity in prior postembedding experiments in other brain regions (Watson & Bazzaz, 2001; Dallvechia-Adams *et al.*, 2002). Specificity of the labeling was further confirmed in the present study by the substantial difference in labeling density within terminals forming symmetric versus asymmetric synapses and by the lack of labeling following omission of the primary antibody. As rabbit primary antibodies were used for both PHAL and GABA, special attention was paid to ensure that osmication during tissue preparation for electron microscopy completely destroyed the antigenicity of the primary antibody directed against PHAL that was incorporated prior to plastic embedding. Consistent with previous reports (Phend *et al.*, 1995), omission of the GABA primary antiserum followed by application of the gold-conjugated anti-rabbit secondary IgG produced no gold particles over PHAL-containing profiles.

For postembedding, sections were collected on nickel grids and dried overnight. Then the grids were placed onto drops of filtered reagents (0.22 μm filter) with the exception that antibody solutions were not filtered. To prevent evaporation of the reagents during prolonged incubations, these steps were performed in a wet chamber kept at room temperature.

After preincubation for 5 min in 0.05 M Tris-buffered saline, pH 7.6, containing 0.1% Triton X-100, the grids were incubated overnight with rabbit anti-GABA primary antibody (1:1,000) in 0.05 M TBS, pH 7.6, containing 0.01% Triton X-100 and 1% BSA. The next day, grids were washed for 50 min in 0.05 M TBS, pH 7.6, containing 0.01% Triton X-100 and 1% BSA and then for 5 min in 0.05 M TBS, pH 8.2, containing 0.1% Triton. Than the grids were placed for 90 min in a 1:25 dilution of 15 nm gold-conjugated goat anti-rabbit IgG (Ted Pella, Redding, CA) in 0.05 M TBS, pH 8.2. After several washes in the last buffer, grids were rinsed in distilled water and counterstained with heavy metal as described earlier.

Ultrastructural Analysis

Systematic examination of VTA sections containing tissue taken from just below the tissue-resin interface was conducted at 18,000X to 20,000X magnification, and digital electron micrographs of PHAL labeled axon terminals were captured. For preembedding analysis of synaptic targets and neurotransmitter phenotype, 5,470,831 μm^2 of tissue was examined from TH-labeled sections, 3,821,625 μm^2 was examined from GABA-labeled tissue, and 613,319 μm^2 was examined from VGlut2-labeled material. For postembedding analysis of GABA immunolabeling within LHb axons, 1,121,519 μm^2 was examined from tissue in which PHAL was labeled by preembedding immunogold-silver.

The criteria to establish specific preembedding immunolabeling were the same as previously described (Carr & Sesack, 2000; Omelchenko & Sesack, 2005; 2007). Peroxidase reaction product was detected as an electron-dense precipitate with a flocculent quality. Profiles were determined to express specific preembedding immunogold-silver if they contained 3 or more gold particles. The vast majority of profiles contained many more than 3 particles. In cases

where gold-silver labeling was limited, serial analysis was used to verify the specificity of labeling using the minimum criterion discussed above. In order to avoid false negatives due to the more limited penetration of preembedding immunogold reagents compared to immunoperoxidase (Sesack *et al.*, 2006), only photographic fields (approximately 13.8 μm^2) that also contained immunogold-silver labeling within the field were analyzed. For postembedding immunolabeling, profiles were considered to be immunoreactive for GABA only if they showed a high concentration of gold particles not associated with mitochondria that exceeded at least 3 times the density of labeling in neighboring terminals forming asymmetric synapses.

The criteria set forth by Peters et al. (Peters *et al.*, 1991) were used to identify neuronal elements in electron micrographs. Axon terminals were distinguished from intervaricose axons by the presence of numerous synaptic vesicles in the former. The presence of parallel membranes, intercleft filaments across the synaptic cleft, and accumulated presynaptic vesicles defined synapses. The relative postsynaptic density thickness (Gray, 1959) was used as the criterion to define either an asymmetric synapse (Gray's type I) in cases where the postsynaptic density was thick, or a symmetric synapse (Gray's type II) in those cases where the postsynaptic density was thin or absent. All instances of LHb axon varicosities apposed to dendrites were examined in 2–4 serial sections in order to increase the likelihood of detecting synaptic specializations.

Results

Light Microscopy

PHAL injection sites within the LHb varied somewhat in their appearance and ranged from having dense cores surrounded by halos of diffuse labeling to having light, diffuse labeling throughout the injection site (Fig. 1). Of the 14 total injections (12 unilateral and 2 bilateral in one rat), 10 were centered either in the medial or lateral LHb or involved both portions. The remaining 4 injection sites included little of the LHb and constituted control cases (see below). One case of LHb injection also appeared to involve slight diffusion into the medial habenula, which probably represents little confound for this study, as a projection from the medial habenula to the VTA has never been convincingly demonstrated (Geisler & Zahm, 2005). Moreover, in the animal with bilateral injections, one site was actually centered in the medial habenula and produced only sparse transport to the VTA; this hemisphere served as a control and was not sampled for electron microscopy. In some cases involving the LHb, tracer diffused up along the pipette into the hippocampus; again, this structure is not known to innervate the VTA. In other LHb cases, diffusion was observed into the underlying parafascicular thalamic nucleus immediately surrounding the fasciculus retroflexus. Although the parafascicular thalamus is reported to innervate the VTA, this is a relatively minor projection (Geisler & Zahm, 2005). Moreover, in one control case in which tracer was deposited solely in the parafascicular thalamus, no transport to the VTA was detected. Hence, we retained the cases in which the LHb injections spread slightly into the parafascicular thalamus. Two additional control cases involved injections of PHAL into the paraventricular or mediodorsal thalamus; these injections did not lead to anterograde transport to the VTA. The 4 injections involving mostly thalamic regions or the medial habenula were removed from the study, leaving ten injections in ten animals for the ultrastructural analysis.

Following PHAL injections in the LHb, labeled axons were traced into the VTA and were observed mainly on the ipsilateral side (Fig. 1). Notably fewer fibers were detected in the contralateral VTA or in the ipsilateral substantia nigra. Within the VTA, the distribution of anterogradely labeled axons was not uniform. In rostral and middle portions, the highest concentration of axons was observed along the sheath of the fasciculus retroflexus and in the paranigral subdivision; fewer axons were observed in the parabrachial region. In more caudal sections of the VTA, PHAL-labeled axons were observed more medially in interfascicular and

caudolinear subregions. Many PHAL-labeled axons had morphological features suggestive of fibers of passage. Nonetheless, some exhibited a beaded appearance (Fig. 1B, insert).

Ultrastructural features of LHb axons in the VTA

In different tissue sets, PHAL transported from the LHb to the VTA was detected by either immunoperoxidase or by immunogold-silver. Immunoperoxidase labeling was observed as a dark flocculent product; immunogold-silver labeling was seen as electron dense granules. Regardless of the labeling method, PHAL was consistently observed within axons.

Consistent with the light microscopic impression, the majority of PHAL-containing LHb profiles in the VTA were unmyelinated axons; occasional myelinated fibers were also seen (Fig. 2A,B). PHAL was detected in a modest number of axon varicosities (Figs. 2–6); these contained mainly small clear vesicles and a few also contained dense-cored vesicles (Fig. 2D), suggesting the presence of neuropeptides. Many labeled axons were apposed to dendrites in the VTA, but only a moderate proportion of LHb varicosities were observed to form synapses (43 out of 274 axons observed at the ultrastructural level, 16%). Some of these synapses had either thickened postsynaptic densities characteristic of asymmetric synapses (Fig. 2C) or thin to absent densities associated with symmetric synapses (Fig. 2D). Surprisingly, many of the synapses formed by LHb axons had intermediate morphological features in which the postsynaptic density did not match the classical thicknesses associated with asymmetric or symmetric types (Figs. 3A, 5A). This was true even when synapses were followed in multiple serial sections or when the specimens were rotated and tilted in the z plane so that synapses were viewed from optimal angles perpendicular to the pre- and postsynaptic densities. These observations raised questions regarding the likely transmitter phenotype of LHb axons within the VTA, given that many glutamate axons in the CNS form predominantly asymmetric synapses.

Phenotypic markers of glutamate and GABA in LHb axons in the VTA

Given that many LHb axons in the VTA did not form synapses with classical asymmetric or symmetric morphology, we examined the presence of VGlut2 or GABA in fibers containing PHAL transported anterogradely from the LHb in two animals. For the study of VGlut2 immunoreactivity, a preembedding dual labeling approach was employed, using the more sensitive immunoperoxidase method (Sesack *et al.*, 2006) to ensure detection of even low levels of VGlut2 and using preembedding immunogold-silver to detect PHAL in LHB terminals. The morphology and synaptology of VGlut2 labeling in the VTA was entirely consistent with our previous observations (Omelchenko & Sesack, 2007), including localization to axons forming primarily asymmetric and occasional symmetric synapses. In this tissue, 40 terminals labeled for PHAL were observed, the majority of which (34; 85%) also contained immunoperoxidase labeling for VGlut2 (Fig. 3A). The remaining terminals were immunonegative for VGlut2, even in fields were VGlut2-positive profiles were observed in the adjacent neuropil (Fig. 3B).

For dual labeling of anterograde tracer and GABA, preembedding immunogold-silver labeling for PHAL was combined with postembedding immunogold labeling for GABA as described in a recent publication from this laboratory (Omelchenko & Sesack, 2009). In the tissue prepared according to this protocol, the pattern of postembedding labeling for GABA matched previous descriptions of the VTA. Of the 26 axon varicosities containing preembedding gold-silver labeling for PHAL, the majority (24, 92%) contained little or no postembedding GABA immunoreactivity despite the presence of specific GABA labeling nearby in the field (Fig. 4A). The remaining two profiles were considered to be dually labeled for PHAL and GABA (Fig. 4B). As shown in Figure 5, the density of postembedding gold particles in PHAL-labeled axons overlaps more with tracer-negative axons forming asymmetric as opposed to symmetric synapses.

Synaptic targets of LHb axons in the VTA

Preembedding immunogold-silver labeling for TH or GABA was observed primarily in dendrites and soma throughout the VTA, consistent with previous descriptions (Carr & Sesack, 2000; Omelchenko & Sesack, 2005; 2007). Occasional axonal labeling for each marker was also seen and was most common in tissue immunostained for GABA, which also appeared in glial processes.

The majority of PHAL-labeled LHb axon terminals in tissue immunoreacted for TH or GABA were observed in apposition to labeled or unlabeled dendrites without forming synaptic specializations (Table 1). The synapses that were observed were infrequent and had asymmetric, symmetric or intermediate morphology. Table 1 presents the data combined across all synapse types. In tissue immunolabeled for TH, 45% (10/22) of PHAL-positive axons synapsed onto dendrites containing immunogold-silver labeling for TH (Fig. 6); the remaining axons contacted unlabeled dendrites.

In tissue immunostained for GABA, 52% of PHAL-positive axons (11/21) synapsed onto dendrites containing immunogold-silver labeling for GABA (Fig. 7). The remaining PHAL-labeled varicosities formed synapses onto unlabeled profiles. A few PHAL-positive axons also exhibited gold-silver labeling for GABA, but these were restricted to the immediate surface of the tissue where it interfaced with plastic embedding.

The unlabeled dendrites postsynaptic to LHb axons might belong to non-DA/non-GABA VTA neurons. However, these targets might also include the more distal portions of the dendritic trees of DA and GABA cells where immunoreactivity is below detection threshold. We therefore measured the short-axis diameter of the dendrites receiving synaptic input from the LHb (Fig. 8). In the TH-labeled tissue set, the TH-immunoreactive dendrites postsynaptic to LHb axons had a mean diameter of 1.05 μm (± 0.69 stdev; n = 10), whereas the unlabeled postsynaptic dendrites had a mean diameter of 0.67 μm (± 0.44 stdev; n = 12). In GABA-labeled tissue, the GABA-immunoreactive dendrites postsynaptic to LHb axons had a mean diameter of 1.16 μm (± 0.40 stdev; n = 11), and the unlabeled postsynaptic dendrites had a mean diameter of 0.59 μm (± 0.39 stdev; n = 10). These sample sizes are rather small for rigorous statistical comparisons. Nevertheless, the unlabeled dendrites innervated by LHb axons in the VTA seem to be smaller on average and to contain more distal profiles, than those immunoreactive for either TH or GABA (Fig. 8). Furthermore, there appears to be no obvious difference in the average sizes of the unlabeled dendrites contacted by LHb axons in the TH and GABA-labeled tissue sets.

Discussion

This study is the first direct ultrastructural analysis of inputs from the LHb to VTA DA and GABA cells. The goal of the study was to characterize the synaptology of the LHb projection, which is a potential source for inhibiting VTA DA cells in response to the absence of expected rewards (Matsumoto & Hikosaka, 2007). The results suggest that the LHb is likely to have only a modest direct influence on VTA neurons, with only a low density of synaptic innervation detected. The projection is predominantly glutamatergic and exhibits no overt selectivity for synapsing onto GABA versus DA cells. The low density of observed synapses together with evidence for monosynaptic contacts onto DA neurons are inconsistent with physiological data indicating a nearly uniform inhibition of VTA DA cells evoked by LHb stimulation (Christoph *et al.*, 1986; Ji & Shepard, 2007; Matsumoto & Hikosaka, 2007). Hence, the discussion of these findings will include consideration of other possible sources of indirect inhibitory influence from the LHb that may mask weaker monosynaptic inputs. Figure 9 illustrates the main points of the study.

Methodological Considerations

As discussed in several prior publications from this laboratory (Carr & Sesack, 2000; Sesack *et al.*, 2006; Omelchenko & Sesack, 2007; Omelchenko & Sesack, 2009), the primary technical limitation for studies combining neuronal tract-tracing and immunoelectron microscopy is the potential for false-negative outcomes. Tract-tracing agents typically do not label all the neurons contributing to a pathway, particularly for a structure like the LHb which extends almost the entire rostro-caudal length of the diencephalon. Furthermore, synapses can be underestimated if varicosities are viewed in only single sections. Incomplete penetration of immunoreagents for tracers or markers of cell phenotype can further contribute to false-negative results. The latter issue was minimized by restricting the analysis to the tissue surface (i.e. interface with plastic embedding) where antibodies have optimal penetration. The analysis of serial sections also served to ensure that synapses and profiles with sparse labeling were not overlooked.

Nevertheless, the problem of false-negatives cannot be avoided completely, and the present data probably do underestimate the full extent of the LHb innervation to the VTA. For example, the unlabeled dendrites receiving LHb synapses appeared to more commonly include distal dendrites where antigen levels may have fallen below detection thresholds. However, the fact that these unlabeled dendrites were of similar diameter in the TH and GABA-immunolabeled tissue sets suggests that the underestimation of distal dendrites was comparable across target populations. Furthermore, the conclusion that the LHb produces only a modest synaptic influence on VTA neurons is based on comparison to studies of other excitatory afferents using the same methodological approach (Carr & Sesack, 2000; Omelchenko & Sesack, 2005).

Ultrastructure of LHb axons within the VTA

Our data are consistent with prior light microscopic tracing studies describing the projection from the LHb to the VTA (Herkenham & Nauta, 1979; Araki *et al.*, 1988; Geisler & Zahm, 2005; Geisler *et al.*, 2007; Kim, 2009). Electron microscopic examination revealed that a significant portion of this pathway consists of fibers passing to more caudal brainstem structures, although such fibers may issue *en passant* connections within the VTA. Candidate targets in the brainstem include the dorsal and median raphe, pontine reticular formation, and mesopontine rostromedial tegmental nucleus (Herkenham & Nauta, 1979; Araki *et al.*, 1988; Jhou *et al.*, 2009). The fact that some LHb axons form synaptic varicosities contacting VTA dendrites is consistent with reports of short latency, potentially monosynaptic responses in this region evoked by LHb stimulation (Christoph *et al.*, 1986; Ji & Shepard, 2007).

The finding of both asymmetric and symmetric synaptic contacts formed by LHb axons in the VTA was rather surprising. Although some GABA cells have been reported (Wang *et al.*, 2006), many LHb neurons appear to be glutamatergic (Fremeau *et al.*, 2001; Herzog *et al.*, 2004; Aizawa *et al.*, 2008) including many of those projecting to the VTA (Geisler *et al.*, 2007). Hence, it was expected that the majority of LHb axons would form asymmetric synapses, as these have been correlated with an excitatory physiology (Carlin *et al.*, 1980). Moreover, the fact that many LHb synapses in the VTA exhibited intermediate characteristics, suggests that for this projection, the morphology of the synaptic connections cannot be used to estimate the probable physiological influence.

Our analysis of VGlut2 and GABA immunoreactivity in LHb axons confirms the prior reports of a dominant glutamate phenotype in the projection to the VTA (Brinschwitz *et al.*, 2005; Geisler *et al.*, 2007). The fact that many of these VGlut2-positive LHb axons formed symmetric or intermediate-type synapses is consistent with our previous report that approximately 10% of all VGlut2-containing axons in the VTA form such synapses (Omelchenko & Sesack, 2007).

The finding of dense-cored vesicles in some LHb axons is also consistent with similar observations for the population of VGlut2-positive axons in the VTA (Omelchenko & Sesack, 2007) and indicates the presence of peptide co-transmitters (Thureson-Klein *et al.*, 1986). Substance P was initially reported in the projections of the LHb (Neckers *et al.*, 1979), but this peptide is now known to be confined to the medial habenula (Ljungdahl *et al.*, 1978; Shinoda *et al.*, 1984; Aizawa *et al.*, 2008). Cells containing neuropeptide Y have been described in the LHb at least in the primate (Smith *et al.*, 1985). Further studies are needed to identify which neuroactive peptides are contained in LHb axons projecting to the VTA, as the presence of dense-cored vesicles reported here suggests that peptides contribute to the physiological regulation of VTA neurons by the LHb.

Targets of LHb axons within the VTA

The apparent lack of selectivity of LHb synapses for GABA as opposed to DA neurons in the VTA is inconsistent with our initial hypothesis. Nevertheless, some LHb synapses onto GABA cells were observed in the present study. Furthermore, our recent report of local collateral connections of GABA neurons to neighboring DA cells (Omelchenko & Sesack, 2009) provides potential anatomical substrates for LHb evoked inhibition of DA neurons (Christoph *et al.*, 1986; Ji & Shepard, 2007; Matsumoto & Hikosaka, 2007). However, this relatively modest circuitry does not explain how LHb stimulation could evoke inhibition, or inhibition followed by delayed excitation, in 97% of all VTA DA neurons recorded *in vivo* (Ji & Shepard, 2007).

The observed synaptic inputs from the LHb to VTA DA cells are also inconsistent with multiple *in vivo* physiological reports that LHb stimulation inhibits these neurons (Christoph *et al.*, 1986; Ji & Shepard, 2007; Matsumoto & Hikosaka, 2007). In this regard, it is interesting to note that one *in vitro* study reported weak excitatory post synaptic potentials (EPSPs) and a limited number of inhibitory post synaptic potentials (IPSPs) in both presumed DA and non-DA cells following electrical stimulation of the LHb (Matsuda & Fujimura, 1992). This study is the only investigation to date that used intracellular recording from an *in vitro* slice preparation that preserved the LHb to VTA connection and allowed detection of subthreshold responses. Indeed, the authors commented that EPSPs typically did not evoke spiking in DA cells (Matsuda & Fujimura, 1992). Based on their findings, one might expect that the innervation of VTA cells by LHb afferents is relatively light and targets both GABA and DA cells with mostly excitatory inputs. This expectation is well matched to the present results. The absence of strong inhibitory responses in the *in vitro* study (Matsuda & Fujimura, 1992) further implies that a critical intermediate structure was not preserved in the slice preparation that was used.

It is premature to conclude that LHb projections exhibit no selectivity for any VTA cell population, given that the analysis did not include a third, minor group of glutamate-containing neurons recently described in this region (Hur & Zaborszky, 2005; Kawano *et al.*, 2006; Yamaguchi *et al.*, 2007; Nair-Roberts *et al.*, 2008). These cells have only been identified on the basis of *in situ* hybridization for VGlut2 mRNA, and this procedure has not yet been reliably adapted for quality ultrastructural studies in the VTA. Hence, future analysis is needed to determine whether VTA glutamate neurons are innervated by axons from the LHb.

Functional significance

The observation of only modest synapses within the VTA suggests that the uniform inhibitory influence mediated by the LHb onto DA cells (Christoph *et al.*, 1986; Ji & Shepard, 2007) involves some other intermediate source of GABA. The most likely candidate for this intermediary is a newly discovered region in the caudal-most VTA that has been called the mesopontine rostromedial tegmental nucleus (RMTg) (Jhou *et al.*, 2009). Importantly, the

RMTg receives substantial innervation from the LHb (Herkenham & Nauta, 1979; Araki *et al.*, 1988; Jhou *et al.*, 2009), contains almost exclusively GABA neurons (Perrotti *et al.*, 2005; Olson & Nestler, 2007), and projects extensively to the entire nigra-VTA complex (Ferreira *et al.*, 2008; Jhou *et al.*, 2009). Together, these observations are likely to account for the ability of LHb output to uniformly inhibit DA neurons in both the substantia nigra and VTA (Christoph *et al.*, 1986; Ji & Shepard, 2007). Moreover, the fact that RMTg neurons can be activated by aversive stimuli suggests that they may inhibit DA neurons under these conditions (Jhou & Gallagher, 2007). Further studies of the RMTg, such as those currently being performed in our laboratory, will be important for testing whether LHb axons synapse onto GABAergic RMTg neurons that in turn innervate the nigra-VTA.

The LHb also innervates other brainstem targets that are afferent to the VTA, including the dorsal raphe nucleus and the mesopontine tegmentum (Herkenham & Nauta, 1979; Araki *et al.*, 1988; Van Bockstaele *et al.*, 1994; Charara *et al.*, 1996; Varga *et al.*, 2003; Omelchenko & Sesack, 2005). It is unclear whether these additional indirect routes can account for the inhibitory influence mediated by the LHb on VTA DA neurons. In the case of the DRN, this seems unlikely, given that the LHb inhibits most serotonin neurons (Wang & Aghajanian, 1977), which in turn are predominantly inhibitory to DA cells in the VTA (Gervais & Rouillard, 2000). Nevertheless, the presence of multiple direct and indirect pathways that connect the LHb to the VTA suggests that the overall functional impact of the LHb on DA cells is likely to be complex.

The physiological function of the direct projection from the LHb to the VTA remains to be established. Studies combining retrograde tract-tracing from forebrain targets such as the nucleus accumbens or prefrontal cortex are needed to determine which populations of VTA DA and GABA cells receive direct synaptic input from the LHb. However, the sparse nature of the monosynaptic LHb to VTA connection makes such experiments challenging. One possible function of the midbrain LHb input is to regulate the modulatory feedback from DA cells to the LHb. However, recent observations indicate that the LHb projects mainly to the posterior VTA, whereas the reciprocal projection arises mainly from the anterior VTA (Gruber *et al.*, 2007). Hence, it is unlikely that the LHb modulates DA neurons that project back to the LHb. Further investigation is needed to elucidate the role of the direct synaptic projections observed in the present study.

Increasing evidence indicates that the LHb plays an important role in regulating reward learning, pain processing, reproductive behavior, sleep-wake cycles, and stress responses (Klemm, 2004; Hikosaka, 2007; Geisler & Trimble, 2008; Hikosaka *et al.*, 2008). Dysregulation of activity in this region may contribute to the pathophysiology of mental disorders such as schizophrenia, depression, and substance abuse (Shepard *et al.*, 2006; Lecourtier & Kelly, 2007; Hikosaka *et al.*, 2008). The direct clinical implications for the present results are as yet unclear. Nevertheless, ultrastructural investigations are important for revealing the exact synaptic connections through which the LHb influences the activity of VTA DA and GABA neurons and regulates the motivated behaviors that are controlled by these cells.

Acknowledgments

Grant support: USPHS grant NIMH 067937

References

Aizawa H, Isomura Y, Kobayasi M, Harukuni R, Tanaka S, Fukai T, Okamoto H. Heterogeneity of the lateral habenular neurons revealed by gene expression. Soc Neurosci Abstr 2008:490–492.

Araki M, McGeer PL, Kimura H. The efferent projections of the rat lateral habenular nucleus revealed by the PHA-L anterograde tracing method. Brain Res 1988;441:319–330. [PubMed: 2451982]

Bell R, Omelchenko N, Sesack SR. Lateral habenula projections to the ventral tegmental area in the rat synapse onto dopamine and GABA neurons. Society for Neuroscience Abstracts 2007:780–789.

Bellocchio EE, Hu H, Pohorille A, Chan J, Pickel VM, Edwards RH. The localization of the brain-specific inorganic phosphate transporter suggests a specific presynaptic role in glutamatergic transmission. J Neurosci 1998;18:8648–8659. [PubMed: 9786972]

Bokor H, Frere SG, Eyre MD, Slezia A, Ulbert I, Luthi A, Acsady L. Selective GABAergic control of higher-order thalamic relays. Neuron 2005;45:929–940. [PubMed: 15797553]

Brinschwitz K, Lommel R, Penkalla A, Goertzen A, Geisler S, Veh RW. Glutamatergic fibers from the lateral habenula do not terminate on dopaminergic neurons in the ventral tegmental area. Soc Neurosci Abstr 2005:891–823.

Brozoski T, Brown R, Rosvold H, Goldman P. Cognitive deficit caused by regional depletion of dopamine in prefrontal cortex of rhesus monkey. Science 1979;205:929–932. [PubMed: 112679]

Carlin RK, Grab DJ, Cohen RS, Siekevitz P. Isolation and characterization of postsynaptic densities from various brain regions: enrichment of different types of postsynaptic densities. J Cell Biol 1980;86:831–843. [PubMed: 7410481]

Carr DB, Sesack SR. Projections from the rat prefrontal cortex to the ventral tegmental area: target specificity in the synaptic associations with mesoaccumbens and mesocortical neurons. J Neurosci 2000;20:3864–3873. [PubMed: 10804226]

Charara A, Smith Y, Parent A. Glutamatergic inputs from the pedunculopontine nucleus to midbrain dopaminergic neurons in primates: *phaseolus vulgaris*-leucoagglutinin anterograde labeling combined with postembedding glutamate and GABA immunohistochemistry. J Comp Neurol 1996;364:254–266. [PubMed: 8788248]

Christoph GR, Leonzio RJ, Wilcox KS. Stimulation of the lateral habenula inhibits dopamine-containing neurons in the substantia nigra and ventral tegmental area of the rat. J Neurosci 1986;6:613–619. [PubMed: 3958786]

Dallvechia-Adams S, Kuhar MJ, Smith Y. Cocaine- and amphetamine-regulated transcript peptide projections in the ventral midbrain: colocalization with gamma-aminobutyric acid, melanin-concentrating hormone, dynorphin, and synaptic interactions with dopamine neurons. J Comp Neurol 2002;448:360–372. [PubMed: 12115699]

Ferreira JG, Del-Fava F, Hasue RH, Shammah-Lagnado SJ. Organization of ventral tegmental area projections to the ventral tegmental area-nigral complex in the rat. Neuroscience 2008;153:196–213. [PubMed: 18358616]

Fremeau RT Jr, Troyer MD, Pahner I, Nygaard GO, Tran CH, Reimer RJ, Bellocchio EE, Fortin D, Storm-Mathisen J, Edwards RH. The expression of vesicular glutamate transporters defines two classes of excitatory synapse. Neuron 2001;31:247–260. [PubMed: 11502256]

Geisler S, Derst C, Veh RW, Zahm DS. Glutamatergic afferents of the ventral tegmental area in the rat. J Neurosci 2007;27:5730–5743. [PubMed: 17522317]

Geisler S, Trimble M. The lateral habenula: no longer neglected. CNS Spectr 2008;13:484–489. [PubMed: 18567972]

Geisler S, Zahm DS. Afferents of the ventral tegmental area in the rat-anatomical substratum for integrative functions. J Comp Neurol 2005;490:270–294. [PubMed: 16082674]

Gervais J, Rouillard C. Dorsal raphe stimulation differentially modulates dopaminergic neurons in the ventral tegmental area and substantia nigra. Synapse 2000;35:281–291. [PubMed: 10657038]

Grace A, Bunney B. Opposing effects of striatonigral feedback pathways on midbrain dopamine cell activity. Brain Res 1985;333:271–284. [PubMed: 2986775]

Grace AA, Floresco SB, Goto Y, Lodge DJ. Regulation of firing of dopaminergic neurons and control of goal-directed behaviors. Trends Neurosci 2007;30:220–227. [PubMed: 17400299]

Gray EG. Axo-somatic and axo-dendritic synapses of the cerebral cortex: an electron microscope study. J Anat 1959;93:420–433. [PubMed: 13829103]

Gruber C, Kahl A, Lebenheim L, Kowski A, Dittgen A, Veh RW. Dopaminergic projections from the VTA substantially contribute to the mesohabenular pathway in the rat. Neurosci Lett 2007;427:165–170. [PubMed: 17949902]

Herkenham M, Nauta WJ. Efferent connections of the habenular nuclei in the rat. J Comp Neurol 1979;187:19–47. [PubMed: 226566]

Herzog E, Gilchrist J, Gras C, Muzerelle A, Ravassard P, Giros B, Gaspar P, El Mestikawy S. Localization of VGLUT3, the vesicular glutamate transporter type 3, in the rat brain. Neuroscience 2004;123:983–1002. [PubMed: 14751290]

Hikosaka, O. Habenula Scholarpedia. 2007. p. 2703

Hikosaka O, Sesack SR, Lecourtier L, Shepard PD. Habenula: crossroad between the basal ganglia and the limbic system. J Neurosci 2008;28:11825–11829. [PubMed: 19005047]

Horvitz JC, Stewart T, Jacobs BL. Burst activity of ventral tegmental dopamine neurons is elicited by sensory stimuli in the awake cat. Brain Res 1997;759:251–258. [PubMed: 9221945]

Hur EE, Zaborszky L. Vglut2 afferents to the medial prefrontal and primary somatosensory cortices: a combined retrograde tracing in situ hybridization. J Comp Neurol 2005;483:351–373. [PubMed: 15682395]

Jhou TC, Gallagher M. Paramedian raphe neurons that project to midbrain dopamine neurons are activated by aversive stimuli. Soc Neurosci Abstr 2007:425–425.

Jhou TC, Geisler S, Marinelli M, Degarmo BA, Zahm DS. The mesopontine rostromedial tegmental nucleus: A structure targeted by the lateral habenula that projects to the ventral tegmental area of Tsai and substantia nigra compacta. J Comp Neurol 2009;513:566–596. [PubMed: 19235216]

Ji H, Shepard PD. Lateral habenula stimulation inhibits rat midbrain dopamine neurons through a GABA (A) receptor-mediated mechanism. J Neurosci 2007;27:6923–6930. [PubMed: 17596440]

Johnson SW, North RA. Two types of neurone in the rat ventral tegmental area and their synaptic inputs. J Physiol 1992;450:455–468. [PubMed: 1331427]

Kalen P, Karlson M, Wiklund L. Possible excitatory amino acid afferents to nucleus raphe dorsalis of the rat investigated with retrograde wheat germ agglutinin and D-[3H]aspartate tracing. Brain Res 1985;360:285–297. [PubMed: 2866825]

Kawano M, Kawasaki A, Sakata-Haga H, Fukui Y, Kawano H, Nogami H, Hisano S. Particular subpopulations of midbrain and hypothalamic dopamine neurons express vesicular glutamate transporter 2 in the rat brain. J Comp Neurol 2006;498:581–592. [PubMed: 16917821]

Kim U. Topographic commissural and descending projections of the habenula in the rat. J Comp Neurol 2009;513:173–187. [PubMed: 19123238]

Kitai ST, Shepard PD, Callaway JC, Scroggs R. Afferent modulation of dopamine neuron firing patterns. Curr Opin Neurobiol 1999;9:690–697. [PubMed: 10607649]

Klemm WR. Habenular and interpeduncularis nuclei: shared components in multiple-function networks. Med Sci Monit 2004;10:RA261–273. [PubMed: 15507867]

Koob GF. Hedonic valence, dopamine and motivation. Mol Psychiatry 1996;1:186–189. [PubMed: 9118342]

Lecourtier L, Defrancesco A, Moghaddam B. Differential tonic influence of lateral habenula on prefrontal cortex and nucleus accumbens dopamine release. Eur J Neurosci 2008;27:1755–1762. [PubMed: 18380670]

Lecourtier L, Kelly PH. A conductor hidden in the orchestra? Role of the habenular complex in monoamine transmission and cognition. Neurosci Biobehav Rev 2007;31:658–672. [PubMed: 17379307]

Lisoprawski A, Herve D, Blanc G, Glowinski J, Tassin JP. Selective activation of the mesocortico-frontal dopaminergic neurons induced by lesion of the habenula in the rat. Brain Res 1980;183:229–234. [PubMed: 7357405]

Ljungdahl A, Hokfelt T, Nilsson G. Distribution of substance P-like immunoreactivity in the central nervous system of the rat - I. Cell bodies and nerve terminals. Neuroscience 1978;3:861–943. [PubMed: 366451]

Matsuda Y, Fujimura K. Action of habenular efferents on ventral tegmental area neurons studied in vitro. Brain Res Bull 1992;28:743–749. [PubMed: 1617458]

Matsumoto M, Hikosaka O. Lateral habenula as a source of negative reward signals in dopamine neurons. Nature 2007;447:1111–1115. [PubMed: 17522629]

Montana V, Ni Y, Sunjara V, Hua X, Parpura V. Vesicular glutamate transporter-dependent glutamate release from astrocytes. J Neurosci 2004;24:2633–2642. [PubMed: 15028755]

Nair-Roberts RG, Chatelain-Badie SD, Benson E, White-Cooper H, Bolam JP, Ungless MA. Stereological estimates of dopaminergic, GABAergic and glutamatergic neurons in the ventral tegmental area, substantia nigra and retrorubral field in the rat. Neuroscience 2008;152:1024–1031. [PubMed: 18355970]

Neckers LM, Schwartz JP, Wyatt RJ, Speciale SG. Substance P afferents from the habenula innervate the dorsal raphe nucleus. Exp Brain Res 1979;37:619–623. [PubMed: 520447]

Nugent FS, Kauer JA. LTP of GABAergic synapses in the ventral tegmental area and beyond. J Physiol 2008;586:1487–1493. [PubMed: 18079157]

Olson VG, Nestler EJ. Topographical organization of GABAergic neurons within the ventral tegmental area of the rat. Synapse 2007;61:87–95. [PubMed: 17117419]

Omelchenko N, Sesack SR. Laterodorsal tegmental projections to identified cell populations in the rat ventral tegmental area. J Comp Neurol 2005;483:217–235. [PubMed: 15678476]

Omelchenko N, Sesack SR. Glutamate synaptic inputs to ventral tegmental area neurons in the rat derive primarily from subcortical sources. Neuroscience 2007;146:1259–1274. [PubMed: 17391856]

Omelchenko N, Sesack SR. Ultrastructural analysis of local collaterals of rat ventral tegmental area neurons: GABA phenotype and synapses onto dopamine and GABA cells. Synapse. 2009 in press.

Overton P, Clark D. Burst firing in midbrain dopaminergic neurons. Brain Res Brain Res Rev 1997;25:312–334. [PubMed: 9495561]

Perrotti LI, Bolanos CA, Choi KH, Russo SJ, Edwards S, Ulery PG, Wallace DL, Self DW, Nestler EJ, Barrot M. DeltaFosB accumulates in a GABAergic cell population in the posterior tail of the ventral tegmental area after psychostimulant treatment. Eur J Neurosci 2005;21:2817–2824. [PubMed: 15926929]

Peters, A.; Palay, SL.; Webster, H. The Fine Structure of the Nervous System: Neurons and Their Supporting Cells. Oxford; New York: 1991.

Phend KD, Rustioni A, Weinberg RJ. An osmium-free method of epon embedment that preserves both ultrastructure and antigenicity for post-embedding immunocytochemistry. J Histochem Cytochem 1995;43:283–292. [PubMed: 7532656]

Phillipson OT. A Golgi study of the ventral tegmental area of Tsai and interfascicular nucleus in the rat. J Comp Neurol 1979;187:99–115. [PubMed: 489780]

Redgrave P, Prescott TJ, Gurney K. Is the short-latency dopamine response too short to signal reward error? Trends Neurosci 1999;22:146–151. [PubMed: 10203849]

Schultz W. Predictive reward signal of dopamine neurons. J Neurophysiol 1998;80:1–27. [PubMed: 9658025]

Sesack, SR.; Miner, LAH.; Omelchenko, N. Pre-embedding immunoelectron microscopy: applications for studies of the nervous system. In: Zaborszky, L.; Wouterlood, F.; Lanciego, J., editors. Neuroanatomical Tract-Tracing 3: Molecules, Neurons, Systems. Springer; New York, NY: 2006. p. 6-71.

Shepard PD, Holcomb HH, Gold JM. Schizophrenia in translation: the presence of absence: habenular regulation of dopamine neurons and the encoding of negative outcomes. Schizophr Bull 2006;32:417–421. [PubMed: 16717257]

Shink E, Smith Y. Differential synaptic innervation of neurons in the internal and external segments of the globus pallidus by the GABA- and glutamate-containing terminals in the squirrel monkey. J Comp Neurol 1995;358:119–141. [PubMed: 7560274]

Shinoda K, Inagaki S, Shiosaka S, Kohno J, Tohyama M. Experimental immunohistochemical studies on the substance P neuron system in the lateral habenular nucleus of the rat: distribution and origins. J Comp Neurol 1984;222:578–588. [PubMed: 6199386]

Smith ID, Grace AA. Role of the subthalamic nucleus in the regulation of nigral dopamine neuron activity. Synapse 1992;12:287–303. [PubMed: 1465742]

Smith Y, Charara A, Parent A. Synaptic innervation of midbrain dopaminergic neurons by glutamate-enriched terminals in the squirrel monkey. J Comp Neurol 1996;364:231–253. [PubMed: 8788247]

Smith Y, Parent A, Kerkerian L, Pelletier G. Distribution of neuropeptide Y immunoreactivity in the basal forebrain and upper brainstem of the squirrel monkey (Saimiri sciureus). J Comp Neurol 1985;236:71–89. [PubMed: 3902914]

Stefani MR, Moghaddam B. Rule learning and reward contingency are associated with dissociable patterns of dopamine activation in the rat prefrontal cortex, nucleus accumbens, and dorsal striatum. J Neurosci 2006;26:8810–8818. [PubMed: 16928870]

Tepper JM, Lee CR. GABAergic control of substantia nigra dopaminergic neurons. Prog Brain Res 2007;160:189–208. [PubMed: 17499115]

Thureson-Klein A, Klein RL, Zhu PC. Exocytosis from large dense cored vesicles as a mechanism for neuropeptide release in the peripheral and central nervous system. Scan Electron Microsc 1986:179–187. [PubMed: 3755544]

Tong ZY, Overton PG, Clark D. Stimulation of the prefrontal cortex in the rat induces patterns of activity in midbrain dopaminergic neurons which resemble natural burst events. Synapse 1996;22:195–208. [PubMed: 9132987]

Ungless MA, Magill PJ, Bolam JP. Uniform inhibition of dopamine neurons in the ventral tegmental area by aversive stimuli. Science 2004;303:2040–2042. [PubMed: 15044807]

Van Bockstaele EJ, Cestari DM, Pickel VM. Synaptic structure and connectivity of serotonin terminals in the ventral tegmental area: potential sites for modulation of mesolimbic dopamine neurons. Brain Res 1994;647:307–322. [PubMed: 7522922]

Van Bockstaele EJ, Pickel VM. GABA-containing neurons in the ventral tegmental area project to the nucleus accumbens in rat brain. Brain Res 1995;682:215–221. [PubMed: 7552315]

Varga V, Kocsis B, Sharp T. Electrophysiological evidence for convergence of inputs from the medial prefrontal cortex and lateral habenula on single neurons in the dorsal raphe nucleus. Eur J Neurosci 2003;17:280–286. [PubMed: 12542664]

Veznedaroglu E, Milner TA. Elimination of artifactual labeling of hippocampal mossy fibers seen following pre-embedding immunogold-silver technique by pretreatment with zinc chelator. Microsc Res Tech 1992;23:100–101. [PubMed: 1327296]

Wang DG, Gong N, Luo B, Xu TL. Absence of GABA type A signaling in adult medial habenular neurons. Neuroscience 2006;141:133–141. [PubMed: 16675141]

Wang RY, Aghajanian GK. Physiological evidence for habenula as major link between forebrain and midbrain raphe. Science 1977;197:89–91. [PubMed: 194312]

Watanabe M, Kodama T, Hikosaka K. Increase of extracellular dopamine in primate prefrontal cortex during a working memory task. J Neurophysiol 1997;78:2795–2798. [PubMed: 9356427]

Watson AH, Bazzaz AA. GABA and glycine-like immunoreactivity at axoaxonic synapses on 1a muscle afferent terminals in the spinal cord of the rat. J Comp Neurol 2001;433:335–348. [PubMed: 11298359]

White FJ. Synaptic regulation of mesocorticolimbic dopamine neurons. Annu Rev Neurosci 1996;19:405–436. [PubMed: 8833449]

Wolf ME, Kapatos G. Flow cytometric analysis and isolation of permeabilized dopamine nerve terminals from rat striatum. J Neurosci 1989;9:106–114. [PubMed: 2563275]

Yamaguchi T, Sheen W, Morales M. Glutamatergic neurons are present in the rat ventral tegmental area. Eur J Neurosci 2007;25:106–118. [PubMed: 17241272]

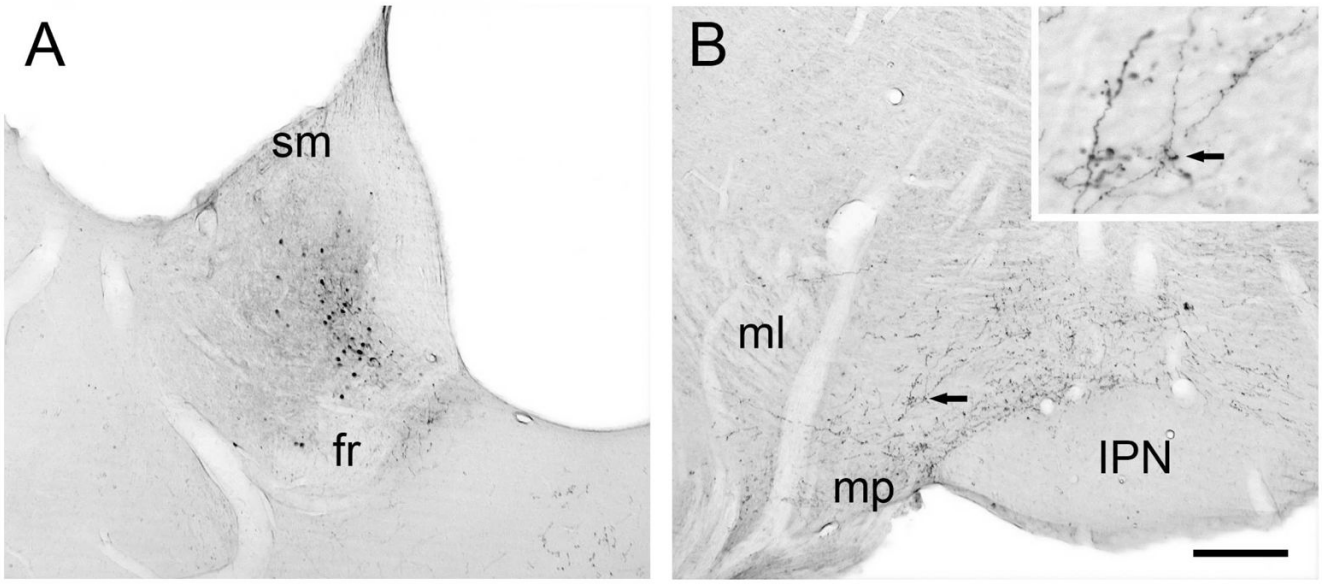

Figure 1.

Light micrographic images of coronal sections through the rat LHb and VTA. Panel A shows the site of PHAL injection contained within the medial division of the LHb, ventral to the stria medullaris (sm) and dorsal to the fasciculus retroflexus (fr). Panel B shows anterograde transport to the VTA bounded by the medial lemniscus (ml), mammillary peduncle (mp), and interpeduncular nucleus (IPN). The black arrow indicates a cluster of beaded axons that is also shown at higher magnification in the insert. Scale bar represents 250 μm for A and B, 50 μm for the insert.

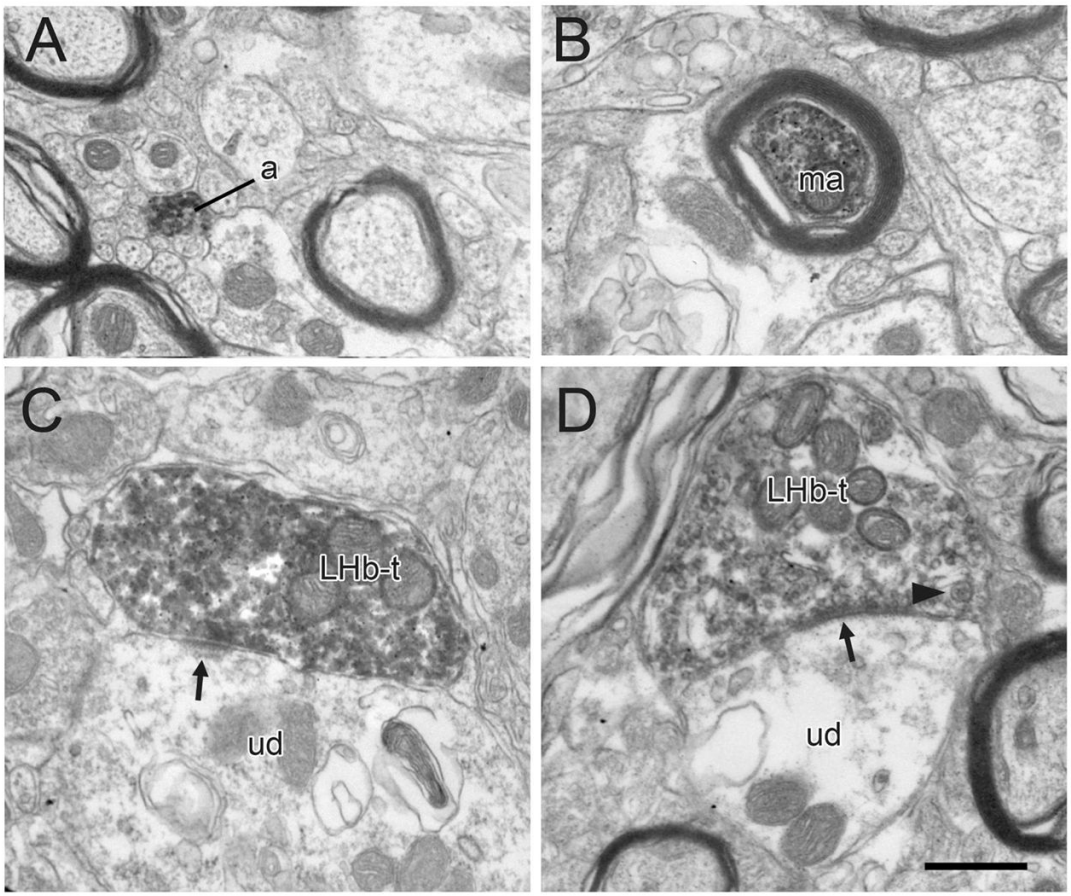

Figure 2.
Electron micrographs showing immunoperoxidase labeling for PHAL transported anterogradely in LHb axons within the rat VTA. The majority of PHAL-labeled profiles are unmyelinated (a) or myelinated (ma) axons passing within bundles of unlabeled axons. Fewer PHAL-labeled profiles are axon terminals (LHb-t) forming asymmetric or symmetric (arrows in C and D, respectively) synaptic specializations onto unlabeled dendrites (ud). The arrowhead in panel D indicates a dense-cored vesicle. Scale bar, 0.5 μm.

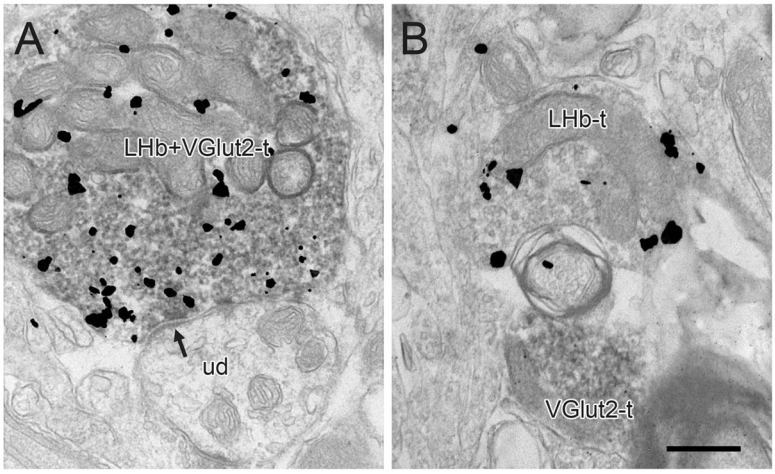

Figure 3.

Electron micrographs of the rat VTA showing immunogold-silver labeling for PHAL in LHb axons in relationship to immunoperoxidase labeling for VGlut2. In A, an axon terminal dually-labeled for both markers (LHb+VGlut2-t) synapses (arrow) onto an unlabeled dendrite (ud). In B, a terminal singly-labeled for PHAL (LHb-t) is positioned next to a VGlut2-labeled profile (VGlut2-t). Scale bar, 0.5 μm.

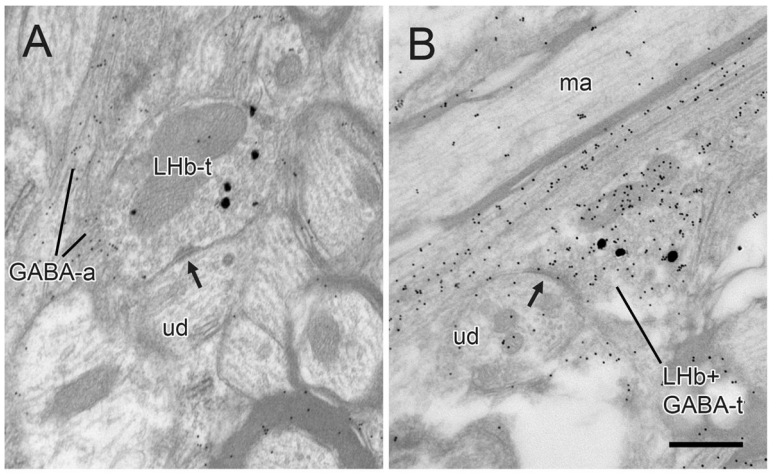

Figure 4.

Electron micrographs of the rat VTA showing preembedding immunogold-silver labeling for PHAL (large, silver-enhanced particles) in LHb axons in relationship to postembedding immunogold labeling for GABA (small, uniform particles). In A, a terminal singly-labeled for PHAL (LHb-t) forms a contact which may be a point of attachment (arrow) onto an unlabeled dendrite (ud). In the adjacent neuropil are small passing axons that are immunoreactive for GABA (GABA-a). In B, a terminal dually-labeled for PHAL and GABA (LHb+GABA-t) forms an apparent synapse (arrow) onto an unlabeled dendrite (ud). An unlabeled myelinated axon (ma) in the adjacent neuropil illustrates the general level of background particles associated with postembedding. Scale bar, 0.5 μm.

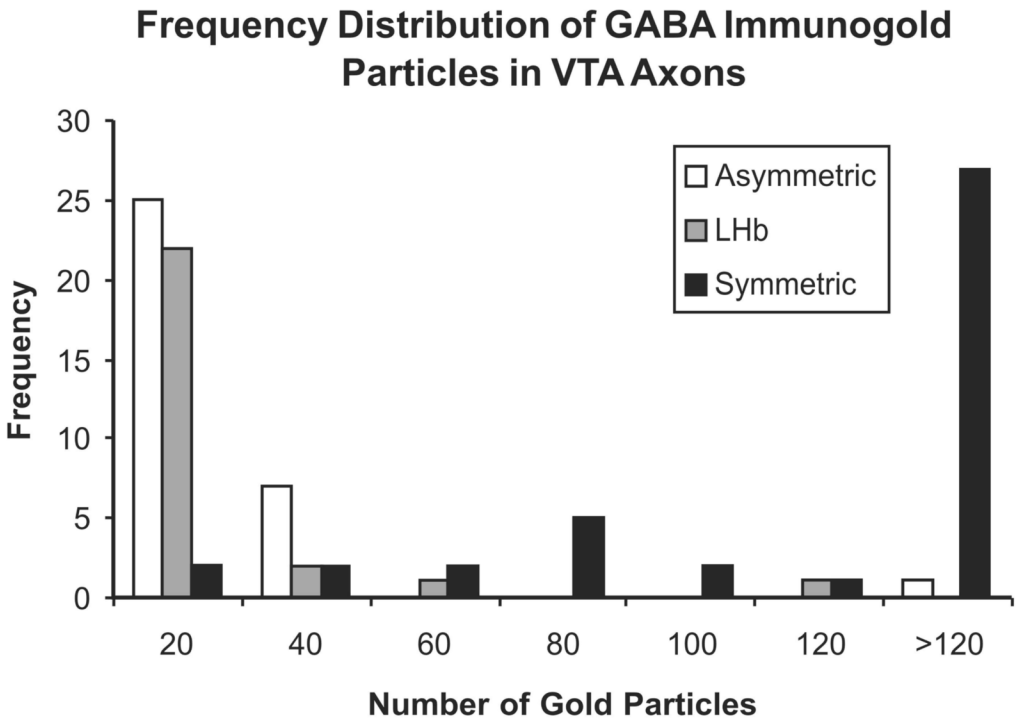

Figure 5.

Frequency histogram illustrating the extent to which LHb axons (gray bars; n = 26) in the VTA contained postembedding immunogold particles for GABA in comparison to tracer-negative axons in the adjacent neuropil forming symmetric (black bars; n = 41) or asymmetric synapses (white bars; n = 33). The bins along the X axis correspond to immunogold particles per axon and range from 0–20, 20–40, 40–60 etc. Two LHb axons with 40–60 and 100–120 gold particles were considered to contain specific GABA labeling; the latter axon is shown in Figure 4.

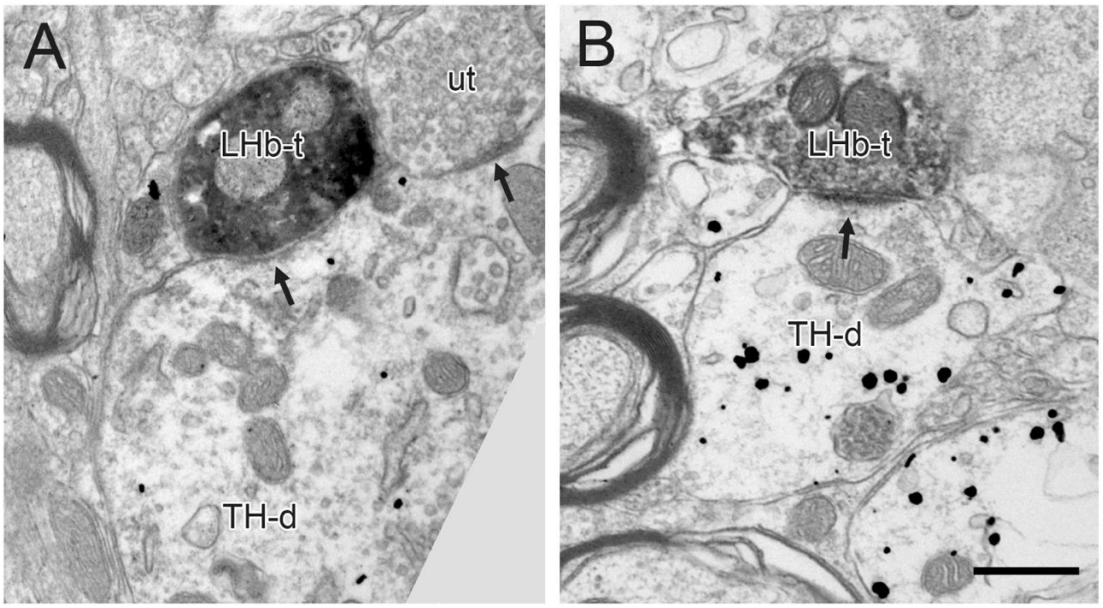

Figure 6.

Electron micrographs showing LHb axons in the VTA containing immunoperoxidase labeling for PHAL and forming synapses (arrows) onto dendrites containing immunogold-silver labeling for TH (TH-d). The synapse in panel A appears to have an intermediate morphology, whereas the synapse in panel B is more typically asymmetric. Commonly, the same dendrites receive additional synaptic inputs from unlabeled terminals (ut). Scale bar, 0.5 μm for A; 0.6 μm for B.

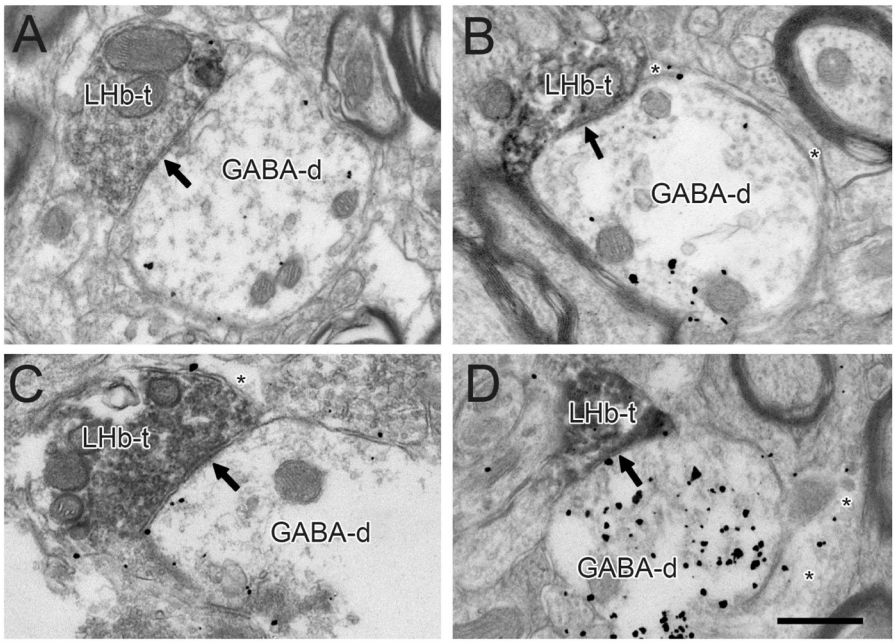

Figure 7.
Electron micrographs showing LHb axon terminals (LHb-t) in the VTA forming synapses (arrows) onto dendrites labeled for GABA (GABA-d). GABA immunoreactivity is also evident in glial processes (asterisks in B-D). Scale bar, 0.5 μm for A, B and D; 0.6 μm for C.

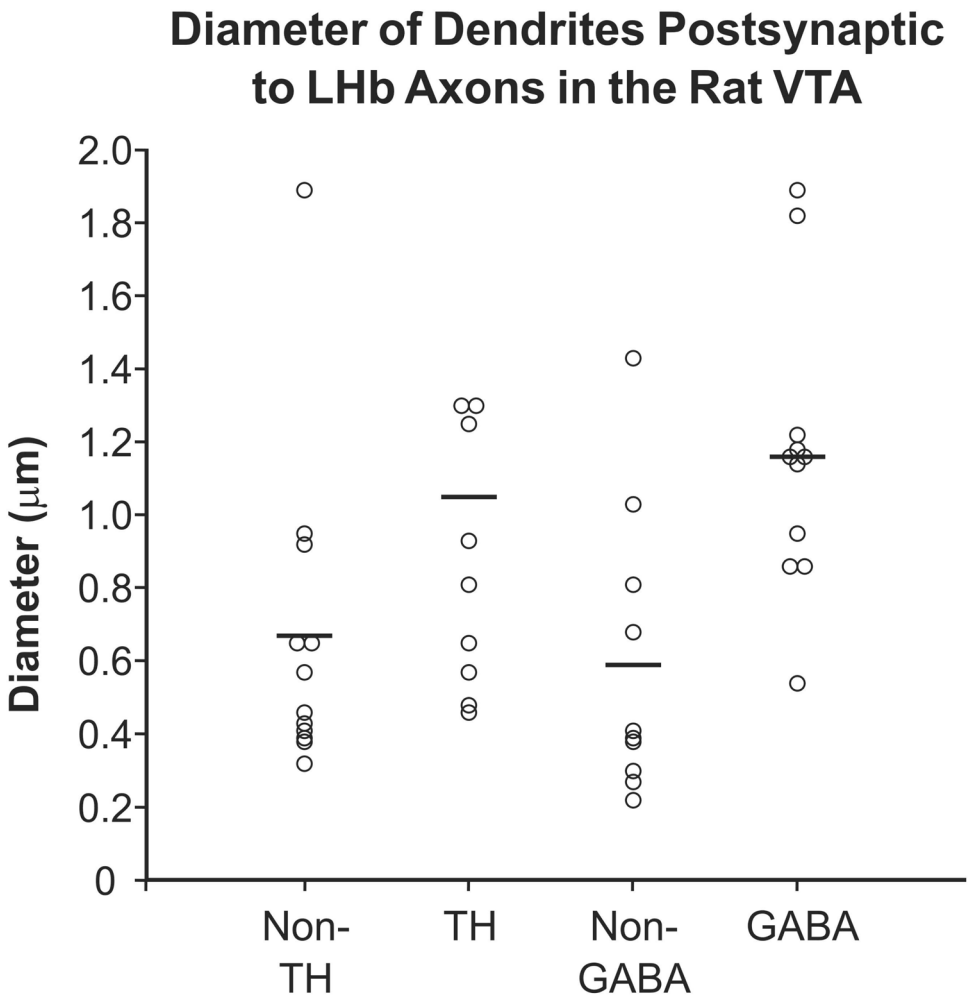

Figure 8.
Scatter plot illustrating the diameter of dendrites in the rat VTA that received synaptic input from LHb axons and were either immunoreactive for TH or GABA or immunonegative for these markers. Horizontal lines indicate the mean diameter for each group. For ease of presentation, the largest diameter dendrite (2.78 μm) in the TH-immunolabeled data set is not included in the plot but was factored into the mean value.

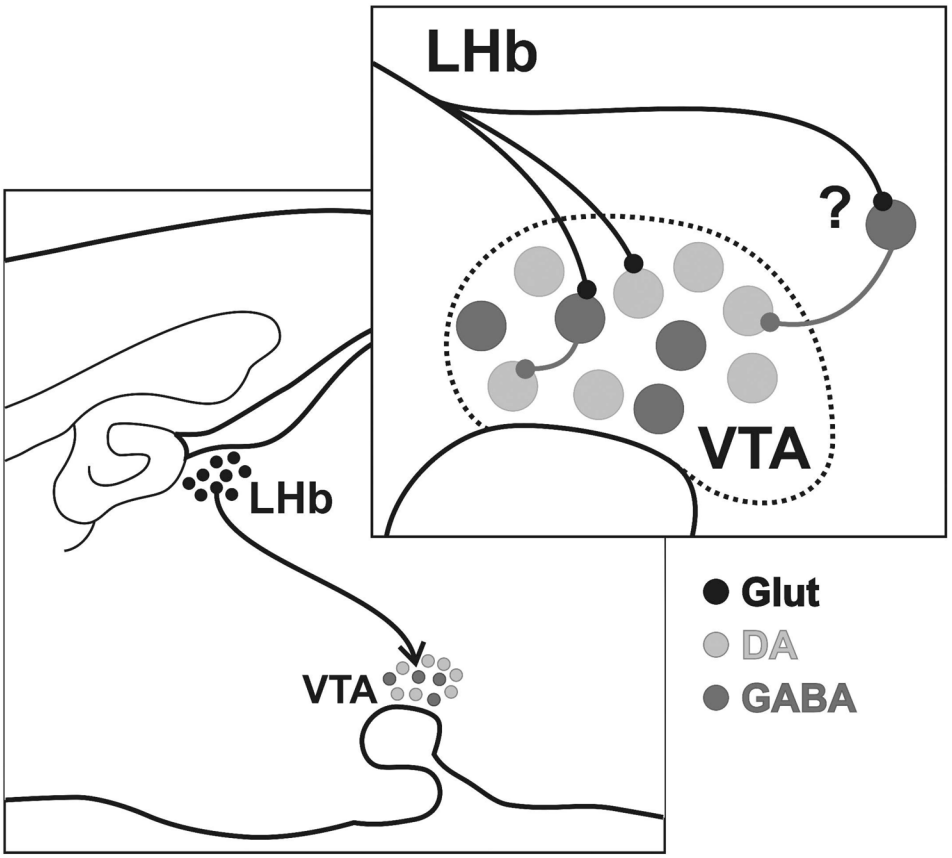

Figure 9.
Schematic diagram illustrating the main findings of the present study. LHb projections to the VTA are predominantly glutamatergic (black) and synapse onto both DA (light gray) and GABA (dark gray) neurons. The latter have been shown to provide local collateral innervation of DA cells. However, the relative infrequency of LHb synapses within the VTA and their lack of selectivity for GABA neurons suggest that an extrinsic source of influence contributes to the uniform inhibition of DA cells evoked by this region.

Table 1

Targets of LHb Axons in the Rat VTA

			Dendrites labeled for:			
Tissue Labeled for TH			**Unlabeled**		**TH**	
total axons	116					
total dendritic contacts*	74	64%	36	49%	38	51%
total synapses	22	30%	12	55%	10	45%
			Dendrites labeled for:			
Tissue Labeled for GABA			**Unlabeled**		**GABA**	
total axons	158					
total dendritic contacts*	75	47%	32	43%	43	57%
total synapses	21	28%	10	48%	11	52%

*dendritic contacts include synapses and appositions